Concentration and desalting of Tetraselmis suecica crude extract by ultrafiltration

Hussein Rida, Jérôme Peydecastaing, Hosni Takache, Ali Ismail, Pierre-Yves
Pontalier

Concentration and desalting of *Tetraselmis suecica* crude extract by ultrafiltration☆

Hussein Rida[a,b,*], Jérôme Peydecastaing[a], Hosni Takache[b,c], Ali Ismail[b], Pierre-Yves Pontalier[a]

[a] *Laboratoire de Chimie Agro-Industrielle (LCA), Université de Toulouse, INRAE, Toulouse INP, 31030 Toulouse, France*
[b] *Platforme de recherche et d'analyses en science de l'environnement (PRASE), Université Libanaise, Hadath, Lebanon*
[c] *Bio-Information Research Laboratory (BIRL), The Higher Institute of Biotechnologies of Paris (Sup'biotech), 66 rue Guy Môquet, 94800 Villejuif, France*

ABSTRACT

Downstream processing, encompassing molecule extraction and extract purification, is a critical step in micro-algal biorefinery. This study focuses on the concentration and desalting of *Tetraselmis suecica* crude extract, which contains proteins, neutral carbohydrates, uronic acids, and pigments. The biomass was initially disrupted with a high-pressure homogenizer operating in moderate conditions (P = 300 bars and 2 passes). The liquid extract obtained was then desalted and concentrated by stirred-cell ultrafiltration. Two membranes, both made of polyethersulfone (PES) but with different molecular weight cut-offs (10 kDa and 30 kDa), were tested for this purpose. The filtration process lasted 3.15 ± 0.34 h, with the temperature maintained at 28 ± 3ºC. There was, therefore, a compelling need to reduce the ash content to facilitate valorization of the extracted proteins. Both membranes displayed time-dependent decreases in permeate flux, membrane permeability, and shear rate. The protein concentration of the permeate increased steadily over time, whereas the concentrations of ash and uronic acids remained constant during ultrafiltration. These results demonstrated the efficacy of both membranes for desalting the extract. After disruption, the ash content in the extract was initially high, at 35.5 ± 0.8% dry weight (DW), decreasing protein purity to 26.1 ± 0.3% DW. The 10 kDa membrane displayed superior molecule retention, resulting in an increase of protein concentration to 50 g.L^{-1} in the final retentate. The 10 kDa membrane eliminated 79.5 ± 0.5% of salts from the extract, potentially achieving the complete retention of proteins, pigments, and uronic acids; approximately 21.4 ± 3.6% of total carbohydrates were removed by this membrane.

1. Introduction

Interest in microalgae is growing, due to their ability to accumulate biomolecules, which constitute a potential feedstock for various industrial applications [1]. These molecules include proteins, carbohydrates, pigments, lipids, and other valuable compounds that can be used for the production of high-value products in the cosmetics, nutrition, and pharmaceutical industries [2]. The processing of microalgae for commercial products and energy generation is known as microalgal biorefinery, and is designed to increase the profitability of the fractionation process [3]. The use of microalgae remains in its infancy, but substantial efforts have been dedicated to establishing a viable biorefinery approach [4]. *Tetraselmis suecica* is a microalga of the class

Chlorophyceae that is up to 12 μm long [5] and known to tolerate a wide range of salt concentrations [6]. It is characterized by a theca, composed of carbohydrate scales, forming an outer cell barrier [7]. This species is one of the most frequently used microalgae, as a feed in aquaculture and in other applications, due to its protein and carbohydrate content [8]. However, approaches for the valorization of biorefinery are still under development.

Microalgal biorefinery is a complex process with two main stages: an upstream stage involving the culture and harvesting of biomass, and a downstream fractionation stage involving cell disruption and purification of the resulting extract [9]. Various techniques for cell disruption [10], separation, and purification [11] are used in microalgal fractionation. Proteins are the target molecules in *Tetraselmis suecica*,

---

Nomenclature

J	Permeate flux
Q_P	Permeate flow rate
S	Membrane surface area
R	Retention rate
VRF	Volume reduction factor
L_p	Membrane permeability
DW	Dry weight.

and the salted solutions in which this microalga is cultured require an additional desalination step for their purification. Several protein desalination methods can be used, including ion-exchange column chromatography and electrodialysis, but ultrafiltration is a more widely used method that is efficient for this purpose [12–14].

Ultrafiltration is a membrane-based separation process for retaining macromolecules [15]. It is used in various phases of microalgal biorefinery, including the harvesting phase [16], but is also widely used for the separation and purification of biomolecules, including proteins in particular [17]. This technique is attractive due to its low cost and high energy efficiency [18], and it has been shown to be useful for the isolation of proteins from plant extracts. Ultrafiltration has, therefore, been studied for the purification of proteins from many crude microalgal extracts. Safi et al. [17] used ultrafiltration to separate and purify water-soluble proteins from *Nannochloropsis gaditana.* They found that enzymatic treatment followed by ultrafiltration with a 300 kDa membrane gave an overall yield of 24.8% in the permeate. Zhou et al. [19] obtained a purity of 70% for *Spirulina* saccharides in the permeate following the use of 4 and 10 kDa ultrafiltration membranes after ultrasound treatment. Gómez-Loredo et al. [20] achieved a recovery rate of 63% for fucoxanthin in the permeate of *Isochrysis galbana* after treatment with alcohol–salt aqueous two-phase systems (ATPS) and by ultrafiltration with a 10 kDa molecular weight cut-off (MWCO) membrane made from regenerated cellulose. Ultrafiltration has already been applied to the concentration and purification of crude extracts of *Tetraselmis suecica*. Garcia et al. [21] reported a protein yield of 26.9% in the retentate of *Tetraselmis suecica* after treatment by bead milling, followed by microfiltration (0.45 μm) and ultrafiltration with 300 kDa and 10 kDa membranes. Jung et al. [22] found that an ultrafiltration membrane made of polyethersulfone (PES) with a MWCO of 150 kDa gave the best performance for the dewatering and concentration of *Tetraselmis suecica* extracts with an initial concentration of 2 g.L⁻¹. Various materials can be used to make ultrafiltration membranes, but PES has emerged as a polymer of choice in ultrafiltration membrane fabrication, particularly for water and wastewater treatment. This polymer has a number of advantages over other materials, including a high glass transition temperature and a high capacity for film formation, rendering it an exemplary material for the production of ultrafiltration membranes with diverse pore sizes and surface areas [23–25]. Furthermore, PES is recognized to be a highly suitable membrane material for diverse separation processes, in the fields of biology, pharmaceuticals, and sterilization in particular [26].

Descriptions of the application of ultrafiltration to *Tetraselmis suecica* after its lysis by high-pressure homogenization (HPH) remain limited. The only reported study on this subject is that by Safi et al. [27], who worked on the fractionation of *Tetraselmis suecica* and purification of the resulting fractions under high-energy conditions, by HPH at 1000 bars followed by a two-stage ultrafiltration process. The proposed process involved the retention of starch and pigments with a 100 kDa membrane in the first step, followed by the separation of proteins from carbohydrates with a 10 kDa membrane. The present work seeks to address a critical gap in current knowledge, by describing the use of moderate conditions to disrupt cells. The structure and composition of the extract are, therefore, different from those in the

previous report, and it was possible to use a single-stage ultrafiltration process to concentrate and desalt the proteins.

Ultrafiltration membranes typically have pore sizes ranging from 0.001 to 0.05 μm, but they are usually characterized by their MWCO, which depends not only on this pore size but also on factors such as solute-membrane interactions, the shape and size of molecules, and the hydrodynamics of the filtration process [28]. However, membrane fouling occurs during ultrafiltration, leading to a decrease in permeate flux, and this fouling depends on the filtration conditions used [19]. Microalgae can be processed by various types of membrane filtration, influenced by several factors. However, for this study, a stirred-cell system was used due to the limited amount of biomass available. A rapid decrease in permeate flux at the start of filtration may result from the formation of a polarization layer. In the context of stirred-cell ultrafiltration, a gel layer of proteins may form, even at concentrations below the solubility limit of the proteins concerned [29]. Solutes are retained by the membrane, whereas the solvent passes through, resulting in the formation of a highly concentrated layer at the membrane interface. Ultimately, the concentration at the membrane interface may reach such a high level that the concentrated solution transforms into a gel with an associated resistance. Gel-layer formation is particularly likely to occur with liquids containing proteins. This deposition may be triggered by various factors, such as aggregation of the proteins present in *Tetraselmis suecica*, even at concentrations below the threshold for gel formation, or precipitation from saturated salt solutions. Interactions between positively and negatively charged proteins can induce aggregation.

A progressive decrease in flux is associated with the changes in viscosity that occur with changes in the concentration of the solution and with progressive membrane fouling. Generally, flux decreases can be attributed to a decrease in the driving force and/or an increase in resistance. Membrane resistance remains constant, but other resistances may emerge due to the blocking of pores by solutes. In addition, the adsorption of solutes onto the walls of the pores in the membrane may decrease membrane permeability. An understanding of these phenomena is crucial for addressing and mitigating flux decline in various filtration scenarios. As the biomass used here is primarily composed of proteins and salts, the selection of inappropriate temperature and pH values for ultrafiltration can lead to a decline in flux through a phenomenon known as scaling. This scaling process may also occur within the membrane itself [30,31].

The primary objective of this study was to investigate the influence of moderate disruption conditions on the concentration and desalting of *Tetraselmis suecica* crude extract in a single-step ultrafiltration process. This investigation focused on proteins, as proteins are the target metabolites for various applications. Following the extraction process, the proteins in the crude extract were found to be associated with large amounts of salts, but also with pigments and polysaccharides, necessitating studies of the removal of these compounds to obtain purified proteins. This study investigated the effect of the MWCO of membranes on separation performances, for selection of the most appropriate membrane for protein desalting and concentration.

2. Materials and methods

2.1. Materials and reagents

Tetraselmis suecica was purchased from Inalve (Nice, France). This strain was produced as a biofilm (patented rotating algal growth system WO2021180713A1) with a dry matter content of 15% to 20%. Fresh biomass was received two days after its harvesting as a concentrated paste. It was stored at 4 °C in the dark and diluted to a concentration of 5% dry weight (DW). Some of the biomass was freeze-dried to prevent rapid degradation before its use for subsequent characterization of total biomolecule content. The rest was diluted three-fold for fractionation. Cell disruption and centrifugation experiments were performed within

24 h of reception of the biomass from the supplier. The Bradford assay kit was purchased from Fisher Scientific, and all chemicals used were of analytical grade and purchased from Sigma Aldrich, France.

2.2. Cell fractionation

Tetraselmis suecica was fractionated in two main steps: cell disruption followed by centrifugation to obtain the liquid extract.

2.2.1. Dilution and cell disruption

The fresh paste was diluted in distilled water to about 5% DW by gentle agitation, at 150 rpm, for 30 min on an orbital shaker. The resulting suspension was then fed into a high-pressure homogenizer (APV-1000 Lab homogenizer (Denmark)) operating at 300 bars and 2 passes. The operating conditions were defined according to the results of a preliminary study (data not shown).

2.2.2. Centrifugation

The homogenate was centrifuged at 10,000 x *g* for 10 min at 20 °C in a Sigma 6–16 K centrifuge (France). A portion of the supernatant was collected for analysis of the liquid fraction, and another portion was freeze-dried in a lyophilizer (Cryonext, France) for further analysis. Most of the remaining supernatant was stored at − 20 °C for six weeks for ultrafiltration experiments. This supernatant is referred to hereafter as the crude extract (CE).

2.3. Ultrafiltration process

The CE was subjected to ultrafiltration in a laboratory-scale Amicon® stirred-cell ultrafiltration unit (Thermo Fisher Scientific, Illkirch, France), with an effective membrane area of 31.17 cm^2 and a volume of 200 mL, as shown in Fig. 1. Compressed air was used to supply a TMP of 2 bars. Two PES membranes with MWCOs of 10 kDa and 30 kDa were used to purify the CE. These membranes are known to be somewhat hydrophilic, thereby mitigating the problem of biocompatibility with proteins [28]. During ultrafiltration, a magnetic stirrer operating at 700 rpm was used to ensure continuous mixing of the CE. Each membrane was used only once and was washed with deionized water before use. Approximately 100 mL of the CE (mean of 99.1 ± 2.6 mL) was initially introduced into the feed tank. It was concentrated by continuous recovery of the permeate until no further permeate flow was observed. The mass of the permeate was continuously monitored over time, and 25 mL samples were collected separately for compositional analysis, to study the variation of permeate composition over time. The retentate obtained at the end of ultrafiltration was also analyzed.

The permeate flux J was calculated based on the permeate flow rate Q_p and the membrane surface area S [27]:

$$J\ (kg.\ h^{-1}.\ m^{-2}) = \frac{Q_p\ \left(\frac{kg}{h}\right)}{S\ \ (m^2)} = \frac{\frac{Permeate\ mass\ (kg)}{time\ (h)}}{S\ (m^2)} \quad (1)$$

The retention rate R was used to characterize the retention of the biomolecules by the membrane [32]:

$$R\ as\ a\% = \left| 1 - \frac{Concentration\ _{biomolecules\ in\ the\ permeate}}{Concentration\ _{biomolecules\ in\ the\ retentate}} \right| \times 100 \quad (2)$$

The concentration of the biomass by ultrafiltration is expressed as the volume reduction factor, VRF, or the volume concentration rate, VCR [32]:

$$VRF = \frac{V_{initial}}{V_{final}} = \frac{V_{initial}}{V_{retentate}} \quad (3)$$

The permeability of the membrane L_p was calculated over time to assess its efficiency [17]:

$$L_p = \frac{Permeate\ volume\ (L)}{time\ (min) \times surface\ area\ (m^2) \times pression\ (bar)} \quad (4)$$

The recovery yield in the permeate was calculated as previously described [33]:

$$yield = \frac{mass\ _{molecule\ in\ the\ permeate}}{mass\ _{molecule\ in\ CE}} \quad (5)$$

2.4. Biochemical analysis

Biochemical analysis was performed on different states of the biomass during the various treatment steps: fresh biomass (DW and ash content), freeze-dried initial biomass (DW, ash content, total proteins, carbohydrates, uronic acids, and FAME), diluted biomass (DW), freeze-dried disrupted biomass (total pigments), supernatant (DW, ash content, total proteins, soluble proteins, carbohydrates, uronic acids, pigments, and FAME), wet retentate (DW, ash content, soluble proteins, carbohydrates, uronic acids, and pigments), freeze-dried retentate (total proteins, carbohydrates, and pigments), liquid permeate (DW, ash content, soluble proteins, uronic acids, and pigments), and freeze-dried permeate (carbohydrates).

Each analytical method is detailed below.

Dry weight was determined gravimetrically after heating the sample in an oven at 103 °C until its weight stabilized. The **ash content** was determined by calcination at 550 °C for 12 h.

For **total protein** biomass analysis and calculation of the extraction yield, proteins were analyzed by the Kjeldahl method with a Kjeltec
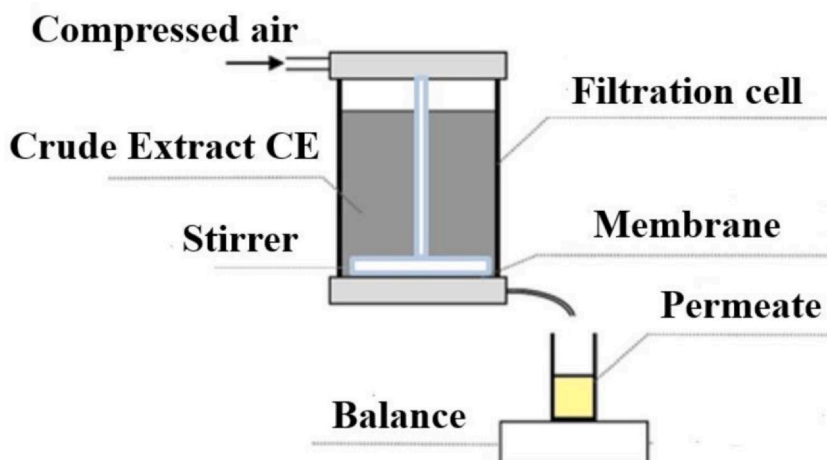

Fig. 1. Schematic diagram of stirred-cell ultrafiltration of the CE.

8400 automatic analyzer and a standard conversion factor (nitrogen to protein) of 5.95 [34]. For the analysis of **soluble proteins** and comparison of the two ultrafiltration membranes, the Bradford method was used, with bovine serum albumin (BSA) as the standard [35].

Carbohydrates were determined according to the protocol of the National Renewable Energy Laboratory (NREL) [36]. In brief, 25 mg of freeze-dried biomass was hydrolyzed with 250 μL of 72% sulfuric acid for 1 h at 30 °C in a water bath. Ultrapure water (7 mL) was then added and the biomass was heated at 121 °C for 1 h in an autoclave. The acidic hydrolysate was allowed to cool and was then neutralized with calcium carbonate, passed through a filter with 0.22-micron pores, and analyzed. The distribution of monosaccharides was determined by high-performance ion chromatography with an HPIC DIONEX ICS 3000 DC-EG equipped with a Carbo-Pac PA-1 column, a post-column equilibrated with 300 mM NaOH, and an AS3000 automatic sampler. The device was equipped with a pulsed electrochemical detector.

Uronic acids were analyzed by the Blumenkrantz titration method [37]. The biomass was hydrolyzed by heating for 5 min at 100 °C with a solution of sodium tetraborate in sulfuric acid. The samples were allowed to cool, a basic solution of 3-metahydroxybiphenyl was added, and absorption was recorded at 520 nm. The concentration of uronic acids was determined by comparison with a calibration curve obtained with the galacturonic acid standard. Uronic acid content is reported on a dry weight basis, as follows:

$$\%Uronic\ acid = \frac{Concentration \times V_{reactant+H_2SO_4}}{m_{sample} \times \%DW} \times 100 \qquad (6)$$

Total pigments (fucoxanthin, lutein, chlorophyll *a*, chlorophyll *b*, and β-carotene) were extracted from freeze-dried biomass according to the protocol of a slightly modified version of the NREL protocol. The fresh biomass was disrupted by HPH at a pressure of 300 bars and 2 passes and immediately freeze-dried. A mixture of 100 μL purified water and 15 mg dried lysate were mixed, vortexed for 15 s, and stored on ice for 30 min to limit biological activity during rehydration. After 30 min, 0.5 mL methanol was added, followed by 0.5 mL chloroform, with vortexing for 15 s after each addition. The samples were centrifuged at 5000 RCF for 5 min, and the supernatant was recovered in another vial. Methanol/chloroform extraction was repeated until the supernatant became transparent. The recovered supernatants were then dried under a gentle stream of clean nitrogen gas and the residue obtained was redissolved in 1 mL methanol: acetone (8:2 v/v). Finally, the dissolved samples were passed through a 0.22 μm-pore polytetrafluoroethylene (PTFE) syringe filter and transferred to high-performance liquid chromatography HPLC vials for analysis.

For freeze-dried samples (supernatant and retentate), 3 mL methanol was added to 20 mg freeze-dried sample in a light-proof vial, which was then incubated in an ultrasound bath for 5 min with shaking. The contents of the vial were then passed through a 0.22 μm-pore PTFE syringe filter and transferred to HPLC vials. For permeates, the amounts recovered were too small for analyses to be performed on freeze-dried samples. Pigment extraction was performed on the liquid permeate and the liquid supernatant (for comparison with dried supernatant) as described by Safi et al. [27].

Pigment analysis was performed by HPLC with a Dionex UltiMate™ 3000 quaternary pump (Thermo Scientific, Massachusetts, USA) and a C18 column (150 mm × 4.6 mm inner diameter, 5 μm particle size, Agilent, France). Pigments were eluted with acetone: methanol: water (55:25:20) at a flow rate of 1 mL.min⁻¹.

Fatty-acid methyl esters (**FAME)** analysis was performed on both the total biomass and the supernatant, to estimate the true potential fuel yield of *Tetraselmis suecica*. FAME analysis was performed by a simple one-step, in situ transesterification method [35,36]. Whole biomass (30 mg) or dried supernatant (50 mg) was solubilized in 1 mL tert-butyl methyl ether (TBME) in the presence of methyl pentadecanoate (C15-FAME) as an internal standard. For in situ transesterification, 300 μL

trimethylsulfonium hydroxide (TMSH; 0.2 M in methanol) was introduced into the vial, which was briefly vortexed. For the extraction of FAME products, 400 μL cyclohexane was added to the vial, which was then vigorously vortexed and allowed to sit at room temperature for 15 - 30 min for decantation. Once the phases had separated, 100 μL of the upper hexane phase containing the FAMEs was analyzed without further purification on a CP-select CB column (50 m long, 0.25 mm internal diameter, 0.25 μm film thickness), with helium as the carrier gas, at a flow rate of 1.2 mL·min⁻¹. The split injector (1:10) and flame ionization detector (FID) were maintained at 250 °C. The oven was set to an initial temperature of 185 °C. It was kept at this temperature for 40 min, and the temperature was then increased to 250 °C at a rate of 15 °C·min⁻¹, and maintained at this temperature for 10.68 min

2.5. Expression of the results and statistical analysis

All experiments were conducted in triplicate, and each sample was analyzed at least twice. All analysis and characterization data are presented as the mean values ± standard deviations of three experiments. One-way ANOVA was performed in Microsoft Excel 2019 for statistical analysis. The results were reproducible to within ± 5% of the mean values.

The total protein content of the retentate was analyzed twice for one replicate as too little material was available for separate analyses for each experiment.

3. Results and discussion

3.1. Extract characterization

The fresh *Tetraselmis suecica* paste was diluted to a concentration of 5.65 ± 0.05% DW and subjected to disruption. The dry matter extraction yield of the CE was 52.1 ± 1.7%, resulting in a dry matter concentration of 32 g.L⁻¹. The DW content of the supernatant serves as an indicator of the degree of cell disruption, corresponding to the extracted biomolecules migrating into the supernatant during centrifugation.

Total protein content was 23.1 ± 0.3% of the DW of the initial biomass according to the Kjeldahl method. Disrupting *Tetraselmis suecica* by HPH increased the total protein content in the CE to 26.1 ± 0.3% DW. Furthermore, the protein extraction yield differed significantly ($p < 0.01$), reaching 61.9 ± 3.9%. Approximately half the extracted proteins were soluble, with a purity of 12.5 ± 0.2% DW of the total biomass. This yield is lower than that reported by Delran et al. [38], who achieved an extraction yield of 80% of total protein by HPH at 400 bars. However, in the latter case, they subjected the initial biomass to a desalting step that may have facilitated protein extraction. This desalting protocol involved the dilution of the biofilm with sodium chloride (NaCl), followed by centrifugation. The supernatant, which contains most of the washed minerals and some lost extracellular components, such as proteins and carbohydrates, was discarded. The pellet was considered to correspond to the initial biomass, and the extraction yield was calculated based on this portion of the biomass. The lower initial biomass protein content used for the calculation would have contributed to a higher extraction yield. Furthermore, the difference in yields may also be due to the efficiency of the HPH equipment used, as different homogenizers can give different results. Safi et al. [27] used a pressure of 1000 bars to disrupt the cells of *Tetraselmis suecica* before the sequential fractionation of biomolecules. The pressure applied in the study reported here has the advantage of lower energy consumption than previously published procedures.

The initial biomass had a relatively high ash content, at 29.6 ± 0.6% DW, possibly due to culture in a saline environment, one of the main nutritional requirements for the growth of *Tetraselmis suecica* [6]. Ash content increased to 35.5 ± 0.8% DW in the CE, primarily due to the hydrophilic nature of the minerals and their high solubility in

Table 1
Pigment content in the initial biomass expressed as % DW. The results shown are the means of three replicates ± SD (n = 3).

Pigment	Fucoxanthin	Lutein	Chlorophyll *b*	Chlorophyll *a*	β-carotene
Content in % DW	0.04 ± 0.004	0.13 ± 0.011	0.03 ± 0.004	0.05 ± 0.005	0.06 ± 0.006

water. This high salt content of the CE decreases the purity of other molecules of value for industrial applications. There is therefore a need for a desalting step to make the CE more suitable for valorization.

The total carbohydrate analysis showed that carbohydrates accounted for 7.3 ± 0.7% DW in the initial biomass. The monosaccharides identified were mannitol, fucose, arabinose, galactose, glucose, mannose, and ribose, consistent with the findings of Pereira et al. [39]. A similar extraction yield ($p > 0.05$) of 35% was achieved for carbohydrates after HPH, while decreasing the purity of the sugars in the CE (4.8 ± 0.6% DW). Delran et al. [40] obtained a higher extraction yield for carbohydrates (60%) at a pressure of 400 bars. This difference can be attributed to the loss of carbohydrates during the washing of the initial biomass in the desalting phase. Carbohydrates are soluble in water, and the low extraction yield may be due to the attachment of macromolecules to the carbohydrates, causing them to migrate into the pellet during centrifugation. Another possible explanation for this low yield is the low pressure applied, which may not be sufficient for complete solubilization of the carbohydrates, leading to their migration into the pellet during centrifugation.

HPH resulted in the extraction of 20 ± 6% of the total uronic acids present in the initial biomass, constituting 6.4 ± 2% DW in the CE. This low yield may be due to the degradation of galacturonic acid molecules during homogenization, as these molecules are structural monosaccharides located in the cell wall [8]. Furthermore, they may be attached to other components leading to their association with the solid phase during centrifugation. Few studies have focused on the extraction of uronic acids from *Tetraselmis suecica*. Becker et al. [41] found that galacturonic acid accounts for 18–21% of the structural sugars found in the cell wall of *Tetraselmis striata*.

The pigments of *Tetraselmis suecica* analyzed — fucoxanthin, lutein, chlorophyll *b*, chlorophyll *a*, and β-carotene — account for 0.3 ± 0.07% DW in the initial biomass (Table 1). As noted by Patel et al. [42], total pigment levels in green algae tend to decrease significantly with increasing salinity. These authors reported that *Tetraselmis suecica* accumulates approximately 2.8–5.5% chlorophyll and 0.35–1.1% carotenoid in salinity concentrations ranging from 15 to 60 g.L^{-1} NaCl. The *Tetraselmis suecica* strain investigated in this study had a high ash content, consistent with its culture in a highly saline environment. These specific culture conditions may account for the observed lower accumulation of pigments.

The pigments were analyzed in the supernatant, both in its liquid form and after freeze-drying. The results of the two analyses were similar: 0.16 ± 0.04% DW in the liquid supernatant and 0.14 ± 0.02% DW after freeze-drying. This similarity validates the precision and accuracy of the two analytical methods used for pigment analysis. The extraction yield for total pigments following HPH was 25.7 ± 3.4%, which is relatively low. Pigments are lipid-soluble molecules [42] that tend to migrate into the solid phase during centrifugation. However, their presence in the CE may be explained by adsorption onto very small pieces of cell debris that remains in the liquid phase after centrifugation, their presence within small lipid droplets (emulsion), or even their attachment to amphiphilic structures (phospholipids). Pigment extraction is also dependent on the location of these molecules in the cell. The low extraction yield may also be attributed to the low pressure applied, which may not have been sufficient to disrupt the chloroplast and provide access to the pigments present in the interthylakoid space [27]. This hypothesis may also account for the lower extraction yield obtained in this study than in that by Delran et al. [40].

Total fatty acids accounted for 1.1% of the DW of the initial

Table 2
Fatty-acid profile of the crude biomass and supernatant of Tetraselmis suecica. The values shown are the mean percent total fatty acids and the corresponding standard deviation (n = 3).

FAME	Crude biomass (%)	Crude extract (%)
C16:0 palmitic acid	31.8 ± 0.2	25.8 ± 0.2
C17:0 heptadecanoic acid	0.3 ± 0.1	1.0 ± 0.4
C18:0 stearic acid	2.0 ± 0.1	2.2 ± 0.1
Total saturated fatty acids ΣSFA	**34.0 ± 0.2**	**28.9 ± 0.1**
C18:1 n-9 t elaidic acid	8.6 ± 0.4	11.9 ± 0.1
C18:1 n-9 oleic acid	15.5 ± 0.3	12.0 ± 0.3
C18:1 n-7c cis vaccenic acid	6.0 ± 0.4	5.3 ± 0.0
C20:1 n-9 9-eicosenoic acid	1.2 ± 0.0	1.2 ± 0.2
Total monounsaturated fatty acids ΣMUFA	**31.2 ± 0.5**	**30.3 ± 0.3**
C18:2n-6 linoleic acid	11.0 ± 1.2	11.7 ± 0.6
C18:3n-3 α- linolenic acid	17.3 ± 0.3	21.2 ± 0.2
C18:4n-3 stearidonic acid	1.9 ± 0.0	2.3 ± 0.0
C20:4n-6 arachidonic acid	1.4 ± 0.0	1.4 ± 0.1
C20:5n-3 eicosapentaenoic acid	3.3 ± 0.1	4.0 ± 0.2
Total polyunsaturated fatty acids ΣPUFA	**34.8 ± 0.8**	**40.7 ± 0.4**

Tetraselmis suecica biomass. This value is consistent with findings of Volkman et al. [43], who reported that free fatty acids account for 0.8% of the total lipids in *Tetraselmis suecica*. However, total fatty-acid content decreased to 0.7% DW in the CE, with an extraction yield of 34.9 ± 2.1%. This decrease can be attributed to the hydrophobic nature of these molecules and their insolubility in water. Nevertheless, their presence in the aqueous phase may be explained by a mechanism similar to that described above for pigments, based on their adsorption onto cell debris remaining in the supernatant after centrifugation. The fatty-acid profile of the crude biomass and the CE is provided in Table 2.

Palmitic acid, oleic acid, and α-linolenic acids were the predominant fatty acids present, accounting for 65% of the total fatty acids in the crude biomass. These results are consistent with those reported by Pereira et al. [39], who identified these fatty acids as the major fatty acids of *Tetraselmis suecica*, with total PUFA accounting for 36% of total fatty acids.

3.2. Ultrafiltration of the CE

The energy consumption of HPH is directly linked to the pressure applied; this parameter can therefore be used to assess the severity of the conditions [44,45]. The moderate pressure used in this work (300 bars, versus 1000 bars in other published protocols) makes it possible to decrease energy consumption. These changes in conditions have effects on cell lysis, molecule recovery, and the degree of cell structure disintegration, modifying the properties of the extract. Despite the mild HPH conditions used, resulting in a protein extraction yield of 60%, characterization of the CE showed that several other molecules were coextracted, including minerals, pigments, and carbohydrates. Furthermore, the protein content of the feed was 26.1 ± 0.33% DW, a value below the salt content. It is therefore imperative to explore ultrafiltration as a means of removing most of the salts while concentrating the remaining biomolecules.
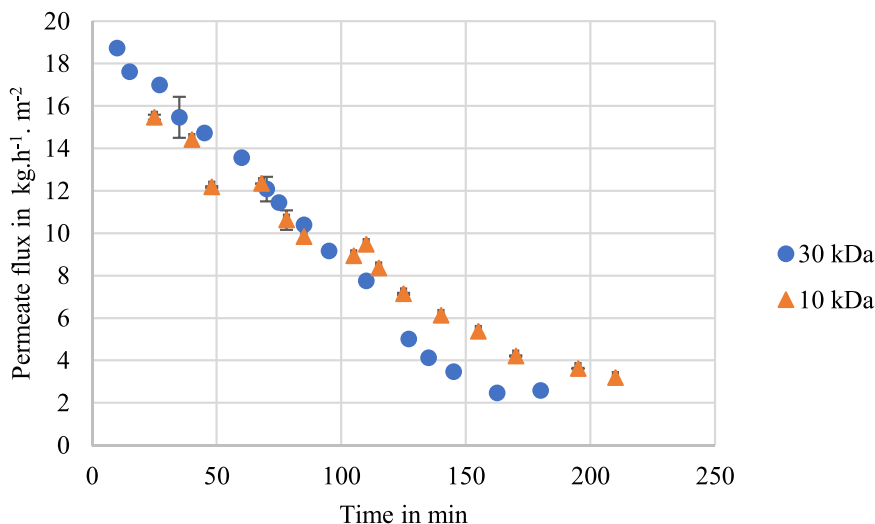
Fig. 2. Variation of permeate flux with filtration time (error bars represent the standard deviation when the points for the three replicates were very close).

3.2.1. Ultrafiltration performance

The two membranes tested for CE ultrafiltration were composed of PES with two different MWCOs: 10 kDa and 30 kDa. For each test, the initial volume used in the unit was 99 ± 2.6 mL of CE with an initial dry matter concentration of 32 g.L⁻¹. The ultrafiltration time for the three repetitions of the two experiments ($n = 6$) was 3.15 ± 0.34 h. Permeate flux decreased with filtration time from 18 ± 0.6 kg.h⁻¹.m⁻² for the 30 kDa membrane and 15.5 ± 0.1 kg.h⁻¹.m⁻² for the 10 kDa membrane to a steady state flux of 2.6 ± 0.6 kg.h⁻¹.m⁻² at the end of filtration for both membranes (Fig. 2).

This decrease in permeate flux has been widely described in previous studies as the permeate flows through the membrane over a period of time, leading to a decrease in the retentate volume (Fig. 3) and, hence, an increase in the concentration and viscosity of the retentate. The decrease was faster for the 30 kDa membrane, probably due to membrane fouling over time, possibly due to the pores becoming blocked by molecules of similar size to the pores of the membrane. Nevertheless, after short periods of filtration (up to approximately 30 min), no significant difference was observed between the two membranes. Fernández and Riera [46] explained this behavior by the formation of a polarization layer at the start of filtration due to the accumulation of biomolecules on the membrane surface, increasing solute concentration in the medium. This accumulation reduces the efficiency of the membrane and accelerates membrane fouling [18]. These findings are consistent with those of Obeid et al. [47], who

observed a similar decrease in permeate flux from 12 to 2 kg/h.m² during the ultrafiltration of *Spirulina sp*. with membranes of two different MWCOs: 10 kDa and 100 kDa.

Membrane behavior can be described as the change in membrane permeability over time. Permeability decreased steadily over time from 0.16 ± 0.008 L.min⁻¹.bar⁻¹.m⁻² to 0.002 L.min⁻¹.bar⁻¹.m⁻² for the 30 kDa membrane and from 0.13 ± 0.02 L.min⁻¹.bar⁻¹.m⁻² to 0.03 ± 002 L.min⁻¹.bar⁻¹.m⁻² for the 10 kDa membrane (Fig. 4).

The tend towards a decrease in permeability can be explained by a steady increase in viscosity leading to a gradual blockage of the membrane pores [17]. Initially, during the early stages of ultrafiltration and up to 70 min, the 30 kDa membrane was more permeable than the 10 kDa membrane. However, at 70 min, the two membranes had similar permeabilities, and the permeability of the 10 kDa membrane exceeded that of the 30 kDa membrane thereafter. These changes in permeability are easier to understand if the ultrafiltration process is split into two phases. The changes can be attributed to two factors: pore size and the assumed change in biomass viscosity over time. During the first phase (before 70 min), pore size played a significant role in solute diffusion through the membranes, with higher rates of diffusion across the 30 kDa membrane than across the 10 kDa membrane. In the second phase (after 70 min), the viscosity of the remaining biomass in the unit was greater in the presence of the 30 kDa membrane than in the presence of the 10 kDa membrane, mainly due to the large volume of liquid in the permeate during the first stage for the 30 kDa membrane than for
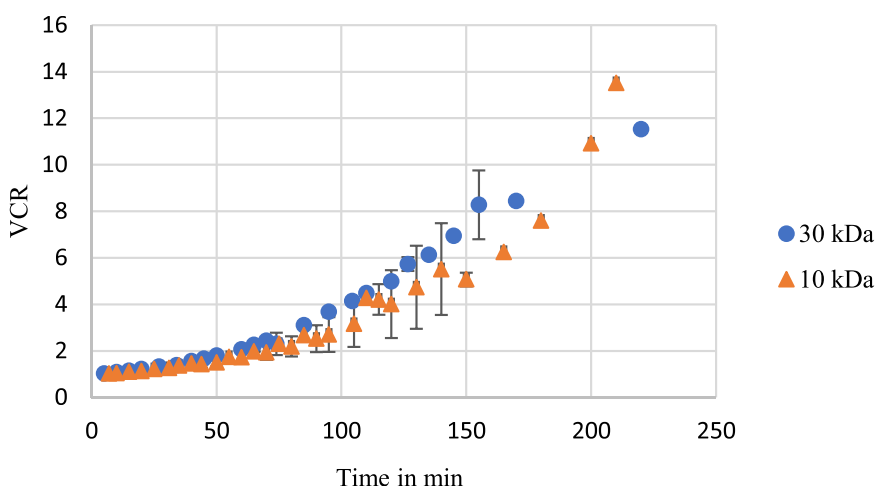

Fig. 3. Change in volume concentration rate (VCR) over time (error bars represent the standard deviation when the points for the three replicates were very close.).
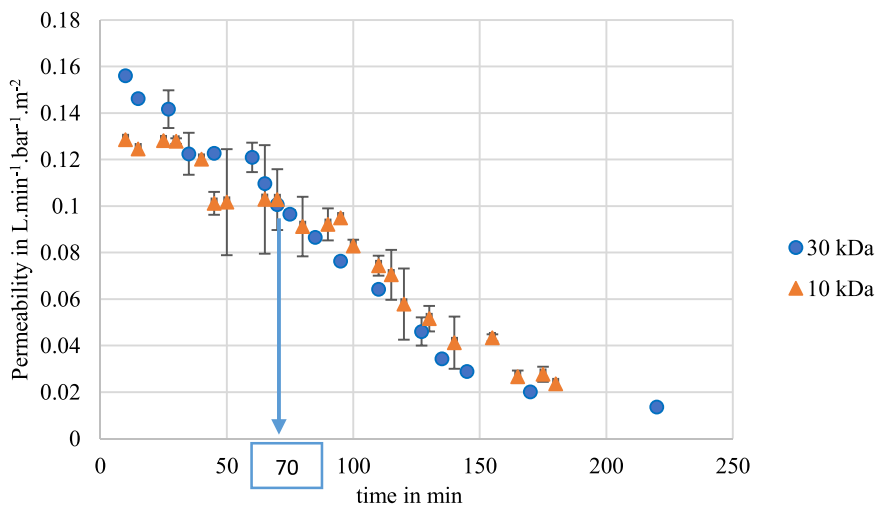
Fig. 4. Change in permeability over time (error bars represent the standard deviation when the points for the three replicates were close.).

the 10 kDa membrane. Safi et al. [17] reported a decrease in membrane permeability over time, with 1000 kDa membrane having a lower permeability than a 300 kDa membrane during 10 h of *Nannochloropsis gaditana* supernatant filtration, following HPH treatment. The decrease in permeability may also be linked to the formation of a polarization layer. Wan Osman et al. [48] attributed this decrease to two factors: membrane fouling and membrane compaction. Membrane fouling occurs when particles or substances accumulate on the surface or in the pores of the membrane, hindering liquid flow through the membrane. The fouling may be due to interactions of proteins and other molecules (mostly lipids and pigments) with the membrane [49]. Conversely, membrane compaction is the physical compression of the membrane itself due to the TMP applied. This phenomenon is closely associated with the hydration state of the membrane, as higher pressures cause the solvent to be expelled.

The shear rates of the two membranes tested decreased with ultrafiltration time (Fig. 5). The trends observed were similar for all three replicates in each experiment. These results explain the decreases in both permeate flux and membrane permeability during ultrafiltration. Shear rate depends on initial biomass viscosity, which increases over time. The formation of a gel layer on the surface weakens the shear forces that allow permeates to pass through the membrane, despite continuous stirring. Darcy's law explains the change in membrane performance over time and attributes the decrease in permeate flux to the increasing viscosity of the medium, assuming that the applied

transmembrane pressure and membrane resistance are constant [50]. Jönsson et al. [51] studied the effect of shear rate on permeate flux and found that the increase in the boundary layer thickness of the retained molecules decreased the shear rate and, consequently, permeate flux. Liu et al. [49] also found that decreases in shear rate led to decrease in permeate flux during ultrafiltration of *Parachlorella kessleri* lysate with a PES membrane.

The primary objective of ultrafiltration was the removal of salts from the CE while maximizing protein concentration, with the ultimate goal of recovering the proteins by drying. This drying process may be constrained by the potential flooding of the dryer with retentate. The findings presented in Figs. 2 and 3 clearly indicate that a VCR of 4 would be the upper limit and would be achieved for a final permeate flow rate of approximately 10 kg.h^{-1}m^{-2}. Further studies are required to determine the changes in the concentrations of the target molecules and to purify and concentrate the proteins.

3.2.2. Retention of molecules

The permeate was recovered separately during ultrafiltration to investigate the changes in its composition over time. The time points chosen for study were based on the recovery of sufficient permeate for the analysis and freeze-drying.

Ultrafiltration of the CE of *Tetraselmis suecica* allowed concentration of the DW from 32 g.L^{-1} to 146.6 $\pm$ 16.2 g.L^{-1} for the 30 kDa membrane and 137 $\pm$ 4.9 g.L^{-1} for the 10 kDa membrane. The recovery yields of
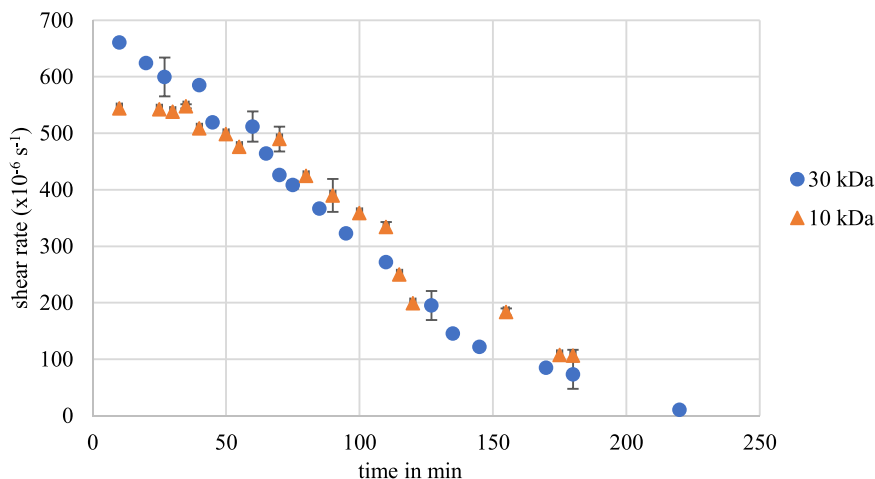

Fig. 5. Changes in shear rate over time (error bars represent the standard deviation when the points for the three replicates were close).

Table 3

Retention rate and mass balance of dry matter and salts for the two membranes, 10 kDa and 30 kDa (results are expressed as the mean value for the three replicates of each experiment (n = 3) ± SD). R_i and R_f were calculated with respect to the initial feed and the retentate, respectively. The desalting rate corresponds to the mass of salt lost in the permeate at each time point.

	Dry matter		Salt	
	30 kDa	10 kDa	30 kDa	10 kDa
Feed concentration in g.L^{-1}	32 ± 3.5	35 ± 2.7	12 ± 0.6	13 ± 0.9
Feed mass in g	3.2 ± 0.3	3.5 ± 0.2	1.1 ± 0.1	1.3 ± 0.1
Retentate concentration in g.L^{-1}	147 ± 16.2	137 ± 4.9	24 ± 2.7	25 ± 1.2
Retentate mass in g	1.3 ± 0.3	1.6 ± 0.1	0.22 ± 0.01	0.3 ± 0.03
Permeate concentration in g.L^{-1}	21 ± 1.2	22 ± 1.5	11 ± 0.4	12 ± 0.9
Permeate mass in g	1.9 ± 0.04	1.9 ± 0.1	0.99 ± 0.1	1.1 ± 0.1
Recovery yield (%)	58.9 ± 4.5	55.1 ± 1.4	89.4 ± 1.4	85.4 ± 5.4
Mean retention rate (%)	85.7 ± 0.8	84.1 ± 0.6	50.3 ± 4.2	50.4 ± 2.4
Initial retention rate at $t = 1$ R_i (%)	40.1 ± 3.9	40.4 ± 4.1	3.9 ± 0.1	12.6 ± 5.2
Final retention rate at $t = 4$ R_f (%)	84.5 ± 1.4	83.9 ± 1.2	52.9 ± 4.2	52.0 ± 4.3
Desalting rate at $t = 1$ (%)	Not applicable		23.6 ± 0.8	23.7 ± 1.9
Desalting rate at $t = 2$ (%)			47.9 ± 1.2	45.8 ± 1.1
Desalting rate at $t = 3$ (%)			72.1 ± 2.2	70.3 ± 4.6
Desalting rate at $t = 4$ (%)			89.4 ± 1.4	85.4 ± 5.4

dry mass in the permeates of the 30 kDa and 10 kDa membranes were 59 ± 1.2% and 58 ± 0.7% respectively, with no losses detected on the basis of material balance. The difference in concentration between the two membranes reflects filtration ending slightly earlier with the 10 kDa membrane. The DW retention rate increased from 40 ± 4% to 84 ± 1%, regardless of the MWCO of the membrane, reflecting the similar performances of the two membranes, with no significant difference between them.

At the end of the concentration step, the Bradford assay analysis of the soluble protein content of the retentate did not provide accurate results, as some of the precipitate did not dissolve. Conversely, there was too little permeate to apply the Kjeldahl method. A material balance was established for the 30 kDa membrane only, with measured and calculated values used to compare the retention rates for total and soluble proteins. Soluble proteins were almost completely retained by the membrane (Table 4), with only a small amount of these proteins recovered in the permeate. This resulted in a negligible loss of soluble proteins (0.4%) and a mean retention rate of 99.6%, giving a theoretical final concentration of 38.78 g.L^{-1} in the concentrate. The final protein concentration in the retentate, as determined by the Kjeldahl method, was 50.9 g.L^{-1} with an initial concentration of 8.72 g.L^{-1} and a mean retention rate of 58%. It can be hypothesized that, during filtration, non-protein molecules containing nitrogen (glucosamine, nucleic acid)

Table 4

Material balance and retention rate for total and soluble proteins with the 30 kDa membrane. (The results for the feed are expressed as the mean values of three replicates.) N/A: Not applicable.

	Feed	Retentate	Permeate
Total protein			
Mass (g)	0.82	0.51	0.31[a]
Concentration (g.L^{-1})	8.72	50.92	3.70
Retention rate (%)	N/A	57.5	N/A
Soluble proteins			
Mass (g)	0.39	0.39[b]	0.00
Concentration (g.L^{-1})	4.17	38.78	0.02
Retention rate (%)	N/A	99.6	N/A
Other molecules[c]			
Mass (g)	0.43	0.12	0.31
Concentration (g.L^{-1})	4.55	12.14	3.68
Retention rate (%)	N/A	19.1	N/A

[a] calculated based on the difference between the protein content for the feed and the retentate determined by the Kjeldahl method.

[b] calculated based on the difference between the protein concentration for the feed and the permeate determined by the Bradford method.

[c] calculated based on the difference between total and soluble protein levels.

were eliminated in the permeate, thereby increasing protein purity.

Permeate protein concentration increased with ultrafiltration time for the membranes tested, although the changes were minimal. Specifically, it increased from 14.6 ± 1.9 µg/mL to 31.2 ± 2.3 µg/mL for the 30 kDa membrane and from 6.5 ± 0.5 µg/mL to 18.8 ± 1.8 µg/mL for the 10 kDa membrane, with BSA as the standard (Fig. 6). The change in protein concentration over time was similar for the two membranes, with no statistically significant difference observed ($p > 0.05$). In previous studies, it was suggested that this behavior results from increasing feed concentration during permeate elimination. Nevertheless, the protein concentration of the permeate can be considered negligible relative to that of the retentate for both membranes (Table 5). Similar results were obtained by Safi et al. [27], who demonstrated complete protein retention for *Tetraselmis suecica* with a PES membrane with a MWCO of 10 kDa at a TMP of 2 bars, following homogenization at 1000 bars. The high rejection rate with the 30 kDa membrane may be due to the formation of a layer that may both enhance membrane selectivity and strongly decrease permeate flux. Proteins play an important role in membrane fouling. These molecules are hydrophobic and are retained by the hydrophilic PES membrane [28]. It has been suggested that membrane fouling, specifically in the form of cake deposition, is independent of the membrane material, but significantly influenced by factors such as the concentration, shape, and size of the microalgae, and the presence of extracellular organic matter [52]. For this process, the membrane with a MWCO of 10 kDa seems to concentrate proteins more efficiently, as it yielded a retentate with a higher protein concentration than that for the 30 kDa membrane.

The ash concentration of the CE was 11 g.L^{-1}, and the mean concentration of ash in the permeate remained constant throughout the ultrafiltration process (Fig. 7). However, the ash concentration in the permeate differed significantly ($p < 0.001$) between the two membranes. Mean retention rate was estimated at 50% at the end of the ultrafiltration process, but the initial rate was about 4% for the 30 kDa membrane and 13% for the 10 kDa membrane, progressively increasing to reach almost 52% for both membranes (Table 3). This change over time explains the increase in the ash concentration to 22 g.L^{-1} in the retentate. Mineral recovery in the permeate was independent of membrane MWCO, with slight differences between the two membranes, possibly due to the heterogeneity of the CE (81.6 ± 6.2% for 30 kDa and 79.5 ± 0.5% for 10 kDa). Minerals are water-soluble molecules, inorganic ion salts characterized by a low molecular weight. Their small size ensures their rapid transfer across the membrane, and their contribution to membrane fouling is negligible as their polarization modulus is very low (< 2). Mineral retention can generally be accounted for by interactions with the larger organic molecules.
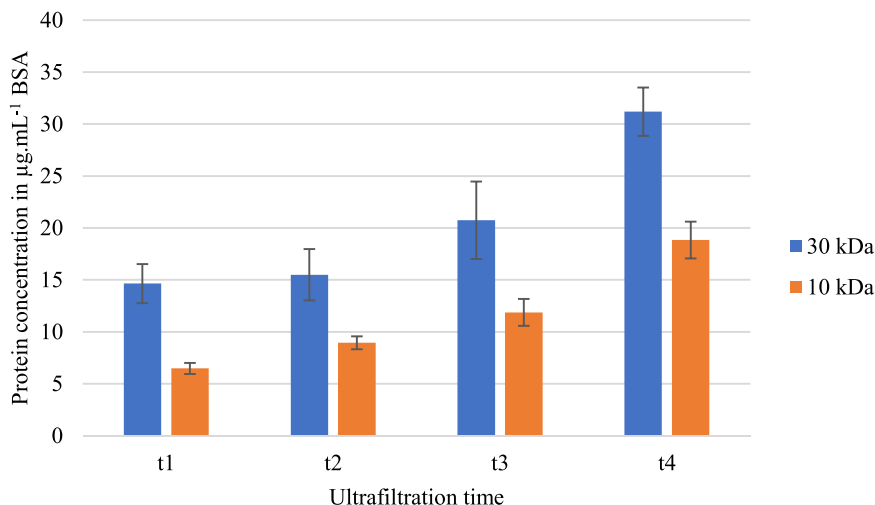
Fig. 6. Changes in the protein concentration of the permeates over time (t1, t2, t3, and t4 correspond to time points at which sufficient volumes of permeate for analysis were recovered). The results are expressed as the mean value for the three replicates.

Table 5
Protein concentration in the permeates and retentates of the 10 kDa and 30 kDa membranes. Results are expressed as the mean value for the three replicates of each experiment (n = 6) ± SD.

Protein concentration ($\mu g.mL^{-1}$) BSA equivalent	Permeate (mean value)	Retentate
30 kDa	19.52 ± 0.93	840.39 ± 147.80
10 kDa	10.03 ± 0.27	1480.95 ± 851.93

The ultrafiltration of *Tetraselmis suecica* CE decreased ash content from 35.5 ± 0.8% DW in the CE to 17.3 ± 1.3% DW in the purified extract for the 30 kDa membrane (the retentate in this case) and to 18.1 ± 0.98% DW for the purified extract for the 10 kDa membrane. The decrease in salt content was not particularly strong because many other molecules were removed at the same time. The demineralization rate reached 89% by the end of ultrafiltration and could be increased by treatment in diafiltration mode.

Despite the high degree of demineralization of the CE, protein purity did not increase considerably during the concentration step (33% DW), due to the retention of other polymers.

Too little permeate was recovered after freeze-drying for determination of the changes in carbohydrate concentration over time. All the freeze-dried permeates were therefore pooled into a sample for analysis. As indicated above, the monosaccharides detected in this strain were mannitol, arabinose, galactose, fucose, glucose, mannose, and ribose, but the detection of these molecules does not necessarily mean that they were present in the monomeric form during filtration. Carbohydrates are heteropolymers containing different fractions of these monomers. The results (Fig. 8) obtained therefore indicate that the carbohydrates present in the initial biomass consisted principally of galactose and mannitol.

Arabinose, fucose, glucose, ribose, and mannose were present at higher concentrations in the retentate than in the permeate, which implies that a large proportion of these molecules was retained by the membranes. Glucose retention rates were higher with the 10 kDa membrane (0.25 ± 0.05 g.L^{-1}) than with the 30 kDa membrane (0.21 ± 0.06 g.L^{-1}). The retention rate for total carbohydrates was generally higher with the 10 kDa membrane (63.1 ± 5.6 5%) than with the 30 kDa membrane (56.3 ± 3.1%). This difference may be explained by some of the monosaccharides having a molecular weight below 30 kDa, resulting in their retention by the 10 kDa membrane but not by the 30 kDa membrane. The recovery rate of these sugars in the
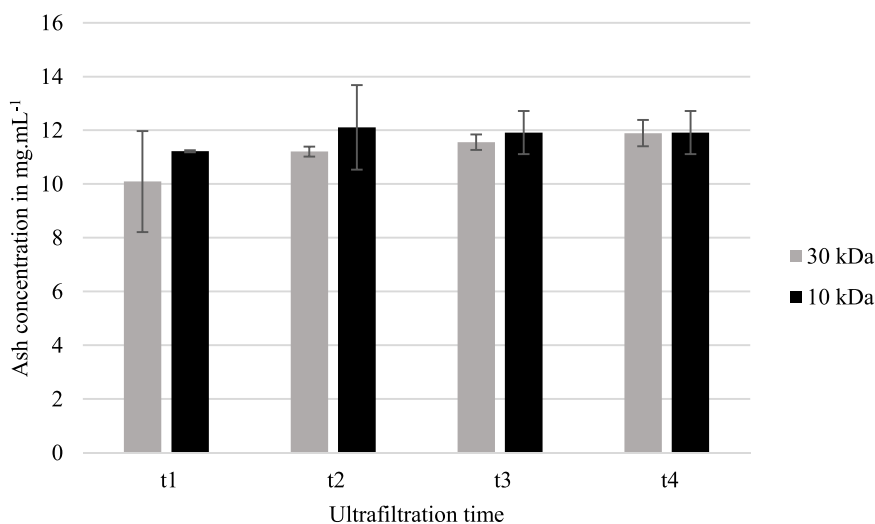
Fig. 7. Change in the ash concentration of the permeate over time (t1, t2, t3, and t4 correspond to time points at which sufficient permeate was recovered for analysis). Results are expressed as the mean value for the three replicates of each experiment (n = 6) ± SD.
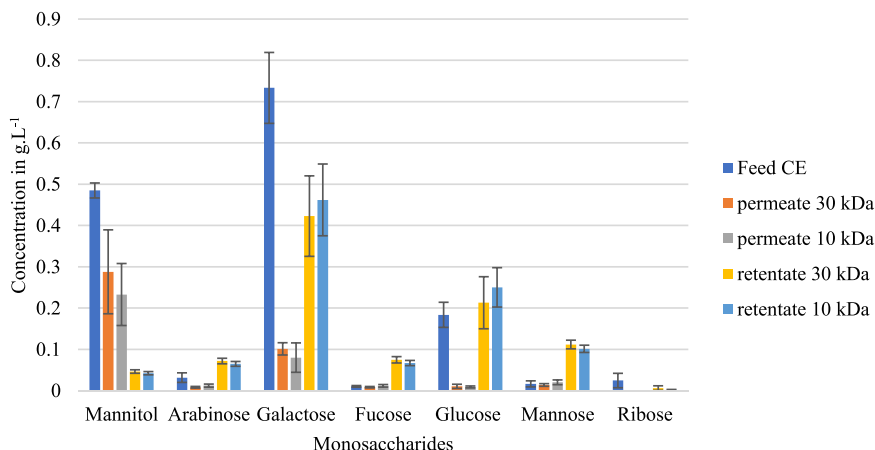
Fig. 8. Monosaccharide composition of the CE, the permeates and retentates of 10 kDa and 30 kDa membranes. Results are expressed as the mean value for the three replicates of each experiment (n = 6) ± SD.

Table 6
Uronic acid concentration in the feed CE, permeates, and retentates of the 10 kDa and 30 kDa membranes. Results are expressed as the mean value for the three replicates of each experiment (n = 6) ± SD.

Concentration (mg.mL^{-1})	Feed CE	Permeate	Retentate
10 kDa	2.03 ± 0.60	0.17 ± 0.05	6.09 ± 1.07
30 kDa		0.13 ± 0.02	5.95 ± 0.88

permeate of the 30 kDa membrane (25.4 ± 6.9%) was higher than that in the permeate of the 10 kDa membrane (21.4 ± 3.6%). Nevertheless, this recovery rate is lower than that obtained by Safi et al. [27], who showed that 65% of saccharides had a molecular weight below 10 kDa. In general, these monosaccharides are water-soluble, and their retention is probably due to their association with large molecules. In this study, carbohydrates were assumed to be present in complexes with other molecules, accounting for their partial retention on the membrane. This retention may be attributed to the low pressure used for HPH, which may have been too low for the release and fragmentation of the polysaccharides. The permeates obtained with both the 30 kDa and 10 kDa membranes contained sugars, but with higher concentrations of mannitol and galactose and low concentrations of glucose and arabinose. This difference in concentration may be explained by structural

form; some of the sugars may have been in oligomeric form, whereas others were monomers. It could be deduced that these sugars are concentrated by ultrafiltration, as for arabinose and glucose. Nevertheless, even if their concentration increases, it would be expected to be higher, given the VCR. Furthermore, the individual mass balance of each sugar was not equilibrated, and it can be deduced that a large amount of these sugars remained on the membrane surface, possibly in the polarization layer, which could contain more polysaccharides than proteins. The fouling phenomenon is a significant drawback of ultrafiltration limiting the feasibility of scaling up this process for large-scale industrial applications. Solute deposition and adsorption on the membrane surface not only decreases permeate flux and modifies the separation efficiency, but also affects the lifetime and durability of the PES membrane. The limitations of polarization layer formation could be overcome by using real tangential filtration at a larger scale and, during the use of the membrane in continuous industrial processes, the membrane could be regular cleaned with chemicals and disinfectants, according to the guidelines provided by the manufacturer. However, this cleaning process can lead to oxidative degradation of the polymers used, decreasing the lifespan of the membrane (referred to as 'membrane aging') and increasing operating costs [53,54]. Various modifications can be made to the membrane to improve its antifouling performance, such as reducing surface roughness, altering surface charge, and adjusting membrane hydrophilicity [55].
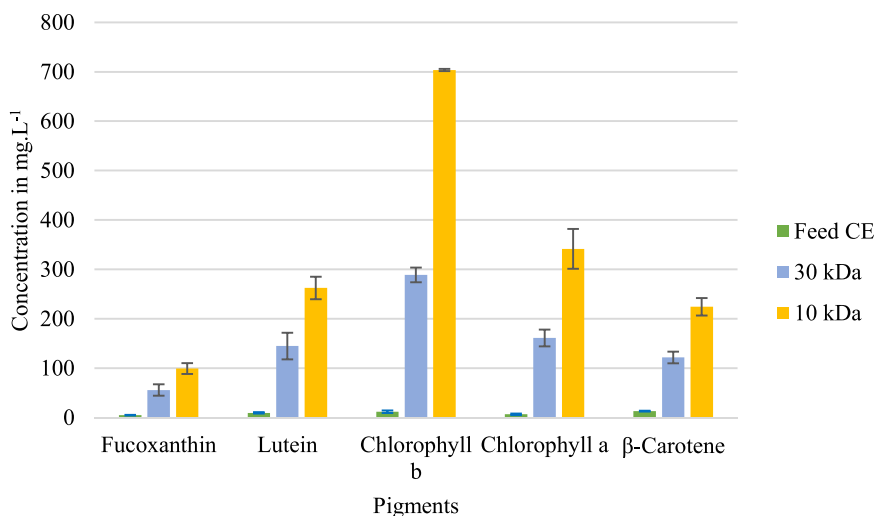

Fig. 9. Pigment contents of the feed and the retentates of the 10 kDa and 30 kDa membranes. Results are expressed as the mean value for the three replicates of each experiment (n = 6) ± SD.

Retention rates were higher for the 10 kDa membrane than for the 30 kDa membrane, which is more suitable for use in protein purification.

Uronic acid concentration in the permeate remained constant during ultrafiltration, behaving similarly to mineral concentration, and the retention rate for uronic acids was 97.5 ± 0.5% regardless of the MWCO of the membrane used (Table 6). One possible explanation for this high retention rate is the attachment of galacturonic acid to other molecules, such as minerals or ash, preventing its diffusion through the membrane. Safi et al. [17] explained the retention of some *Tetraselmis suecica* biomolecules by the formation of complexes of glycoproteins with polysaccharides. In addition, some molecules may infiltrate the membrane pores, subsequently obstructing the membrane and leading to the retention of other molecules within the filtration unit.

All the pigments analyzed were fully retained, as demonstrated by visual observation, as the retentate was green and the permeate was colorless. For a more scientific analysis of the effect of the membrane, the permeate was analyzed in its liquid form, whereas the retentate was analyzed after freeze-drying. The pigments analyzed included fucoxanthin, lutein, chlorophyll *a*, chlorophyll *b*, and β-carotene. No pigments were detected in the permeates of either of the membranes, any peaks being negligible and below the limit of quantification (LOQ). Pigment retention rates were higher with the 10 kDa membrane than with the 30 kDa membrane (Fig. 9), indicating that the 30 kDa membrane would be more suitable for protein purification. Safi et al. [27] reported the complete retention of *Tetraselmis suecica* pigments on a PES membrane with a MWCO of 100 kDa, attributing this retention to the size of the pigment molecules (> 100 kDa) and their presence in emulsions or solid debris that did not settle during centrifugation might contribute to membrane fouling. Total pigment purity increased from 0.14 ± 0.01% DW in the CE to 0.5 ± 0.06% DW in the retentate of the 30 kDa membrane and 1.1 ± 0.1% DW in that of the 10 kDa membrane. Despite the low concentration of pigments, these molecules continue to pose significant challenges in protein utilization due to the intense flavor of chlorophyll. Total pigment removal from proteins is difficult and cannot be achieved by membrane filtration alone.

4. Conclusion

This study compared the performances of two ultrafiltration membranes with MWCOs of 10 and 30 kDa for desalting and concentrating *Tetraselmis suecica* extracts. The results suggest that a high concentration of proteins, up to 50 g.L^{-1}, is possible with both membranes, with minimal protein loss in the permeate. Ultrafiltration simultaneously removed 90% of the salt from the permeate with the 30 kDa membrane and 85% with the 10 kDa membrane. Retention rates were high for both membranes, despite their different MWCOs, probably due to the formation of a fouling and/or polarization layer, leading to low permeate fluxes. The 30 kDa membrane proved more suitable for protein concentration, as it also removed larger amounts of pigment. These tests were performed with stirring, but evaluations of performance in tangential mode are now required. In these conditions, the flow reduces the polarization layer, increasing permeate fluxes, but potentially affecting rejection rate. The significant desalting of the extract suggests that diafiltration may be unnecessary, reducing industrial costs. Ultrafiltration is widely employed for the industrial concentration of plant proteins, and these results highlight the promise of membrane processes for use in protein purification. However, ultrafiltration did not result in a complete removal of pigment. The development of additional methods for depigmentation are therefore required, as these pigments may alter the flavor of the protein.

Declaration of Competing Interest

The authors declare that they have no known competing financial interests or personal relationships that could have appeared to influence the work reported in this paper.

References

[1] Show P-L, Park Y-K, Al-Zuhair S, Ashokkumar V. Guest editorial: special issue on "Microalgae biorefinery: current bottlenecks, challenges, and future directions. Phytochem Rev 2023;22:829–31. https://doi.org/10.1007/s11101-023-09881-0.

[2] Chew KW, Yap JY, Show PL, Suan NH, Juan JC, Ling TC, Lee D-J, Chang J-S. Microalgae biorefinery: high value products perspectives. Bioresour Technol 2017;229:53–62. https://doi.org/10.1016/j.biortech.2017.01.006.

[3] Trivedi J, Aila M, Bangwal DP, Kaul S, Garg MO. Algae based biorefinery—How to make sense? Renew Sustain Energy Rev 2015;47:295–307. https://doi.org/10.1016/j.rser.2015.03.052.

[4] Phong WN, Show PL, Ling TC, Juan JC, Ng E-P, Chang J-S. Mild cell disruption methods for bio-functional proteins recovery from microalgae—Recent developments and future perspectives. Algal Res 2018;31:506–16. https://doi.org/10.1016/j.algal.2017.04.005.

[5] Spiden EM, Yap BHJ, Hill DRA, Kentish SE, Scales PJ, Martin GJO. Quantitative evaluation of the ease of rupture of industrially promising microalgae by high pressure homogenization. Bioresour Technol 2013;140:165–71. https://doi.org/10.1016/j.biortech.2013.04.074.

[6] Fabregas J, Abalde J, Herrero C, Cabezas B, Veiga M. Growth of the marine microalga Tetraselmis suecica in batch cultures with different salinities and nutrient concentrations. Aquaculture 1984;42:207–15. https://doi.org/10.1016/0044-8486(84)90101-7.

[7] Lee AK, Lewis DM, Ashman PJ. Force and energy requirement for microalgal cell disruption: an atomic force microscope evaluation. Bioresour Technol 2013;128:199–206. https://doi.org/10.1016/j.biortech.2012.10.032.

[8] Kermanshahi-pour A, Sommer TJ, Anastas PT, Zimmerman JB. Enzymatic and acid hydrolysis of Tetraselmis suecica for polysaccharide characterization. Bioresour Technol 2014;173:415–21. https://doi.org/10.1016/j.biortech.2014.09.048.

[9] Cai Y, Lim HR, Khoo KS, Ng H-S, Cai Y, Wang J, Tak-Yee Chan A, Show PL. An integration study of microalgae bioactive retention: from microalgae biomass to microalgae bioactives nanoparticle. Food Chem Toxicol 2021;158:112607. https://doi.org/10.1016/j.fct.2021.112607.

[10] Günerken E, D'Hondt E, Eppink MHM, Garcia-Gonzalez L, Elst K, Wijffels RH. Cell disruption for microalgae biorefineries. Biotechnol Adv 2015;33:243–60. https://doi.org/10.1016/j.biotechadv.2015.01.008.

[11] Corrêa PS, Morais Júnior WG, Martins AA, Caetano NS, Mata TM. Microalgae biomolecules: extraction, separation and purification methods. Processes 2020;9:10. https://doi.org/10.3390/pr9010010.

[12] Zhou B, Zhang M, Fang Z, Liu Y. Effects of ultrasound and microwave pretreatments on the ultrafiltration desalination of salted duck egg white protein. Food Bioprod Process 2015;96:306–13. https://doi.org/10.1016/j.fbp.2015.09.004.

[13] Simon A, Vandanjon L, Levesque G, Bourseau P. Concentration and desalination of fish gelatin by ultrafiltration and continuous diafiltration processes. Desalination 2002;144:313–8. https://doi.org/10.1016/S0011-9164(02)00333-8.

[14] Chay Pak Ting BP, Pouliot Y, Juneja LR, Okubo T, Gauthier SF, Mine Y. On the use of ultrafiltration for the concentration and desalting of phosvitin from egg yolk protein concentrate. Int J Food Sci Technol 2010;45:1633–40. https://doi.org/10.1111/j.1365-2621.2010.02311.x.

[15] Baldasso C, Barros TC, Tessaro IC. Concentration and purification of whey proteins by ultrafiltration. Desalination 2011;278:381–6. https://doi.org/10.1016/j.desal.2011.05.055.

[16] Tena FO, Ranglová K, Kubač D, Steinweg C, Thomson C, Masojídek J, Posten C. Characterization of an aerated submerged hollow fiber ultrafiltration device for efficient microalgae harvesting. Eng Life Sci 2021;21:607. https://doi.org/10.1002/elsc.202100052.

[17] Safi C, Olivieri G, Campos RP, Engelen-Smit N, Mulder WJ, van den Broek LAM, Sijtsma L. Biorefinery of microalgal soluble proteins by sequential processing and membrane filtration. Bioresour Technol 2017;225:151–8. https://doi.org/10.1016/j.biortech.2016.11.068.

[18] Liang T, Lu H, Ma J, Sun L, Wang J. Progress on membrane technology for separating bioactive peptides. J Food Eng 2023;340:111321. https://doi.org/10.1016/j.jfoodeng.2022.111321.

[19] Zhou J, Wang M, Barba FJ, Zhu Z, Grimi N. A combined ultrasound + membrane ultrafiltration (USN-UF) process for enhancing saccharides separation from Spirulina (Arthrospira platensis). Innov Food Sci Emerg Technol 2023;85:103341. https://doi.org/10.1016/j.ifset.2023.103341.

[20] Gómez-Loredo A, González-Valdez J, Rito-Palomares M. Insights on the downstream purification of fucoxanthin, a microalgal carotenoid, from an aqueous two-phase system stream exploiting ultrafiltration. J Appl Phycol 2015;27:1517–23. https://doi.org/10.1007/s10811-014-0443-y.

[21] Garcia ES, Van Leeuwen JJA, Safi C, Sijtsma L, Van Den Broek LAM, Eppink MHM, Wijffels RH, Van Den Berg C. Techno-functional properties of crude extracts from the green microalga Tetraselmis suecica. J Agric Food Chem 2018;66:7831–8. https://doi.org/10.1021/acs.jafc.8b01884.

[22] Jung J-Y, Kim K, Choi S-A, Shin H, Kim D, Bai SC, Chang YK, Han J-I. Dynamic filtration with a perforated disk for dewatering of Tetraselmis suecica. Environ Technol 2017;38:3102–8. https://doi.org/10.1080/09593330.2017.1290145.

[23] Arumugham T, Ouda M, Krishnamoorthy R, Hai A, Gnanasundaram N, Hasan SW, Banat F. Surface-engineered polyethersulfone membranes with inherent Fe–Mn bimetallic oxides for improved permeability and antifouling capability. Environ Res 2022;204:112390. https://doi.org/10.1016/j.envres.2021.112390.

[24] Ouda M, Hai A, Krishnamoorthy R, Govindan B, Othman I, Kui CC, Choi MY, Hasan SW, Banat F. Surface tuned polyethersulfone membrane using an iron oxide functionalized halloysite nanocomposite for enhanced humic acid removal. Environ Res 2022;204:112113. https://doi.org/10.1016/j.envres.2021.112113.

[25] Luque-Alled JM, Abdel-Karim A, Alberto M, Leaper S, Perez-Page M, Huang K, Vijayaraghavan A, El-Kalliny AS, Holmes SM, Gorgojo P. Polyethersulfone membranes: from ultrafiltration to nanofiltration via the incorporation of APTS functionalized-graphene oxide. Sep Purif Technol 2020;230:115836. https://doi.org/10.1016/j.seppur.2019.115836.

[26] Rambabu K, Velu S. Improved performance of CaCl2 incorporated polyethersulfone ultrafiltration membranes. Period Polytech Chem Eng 2016;60:181–91. https://doi.org/10.3311/PPch.8482.

[27] Safi C, Liu DZ, Yap BHJ, Martin GJO, Vaca-Garcia C, Pontalier P-Y. A two-stage ultrafiltration process for separating multiple components of Tetraselmis suecica after cell disruption. J Appl Phycol 2014;26:2379–87. https://doi.org/10.1007/s10811-014-0271-0.

[28] Singh R. Membrane Technology and Engineering for Water Purification: Application, Systems Design and Operation. Oxford: Butterworth-Heinemann,; 2014.

[29] Afonso A, Miranda JM, Campos JBLM. Numerical study of BSA ultrafiltration in the limiting flux regime — Effect of variable physical properties. Desalination 2009;249:1139–50. https://doi.org/10.1016/j.desal.2009.05.012.

[30] Van Den Berg GB, Smolders CA. Flux decline in ultrafiltration processes. Desalination 1990;77:101–33. https://doi.org/10.1016/0011-9164(90)85023-4.

[31] Marshall AD, Munro PA, Trägårdh G. The effect of protein fouling in microfiltration and ultrafiltration on permeate flux, protein retention and selectivity: a literature review. Desalination 1993;91:65–108. https://doi.org/10.1016/0011-9164(93)80047-Q.

[32] Oriez V, Pham NT-T, Peydecastaing J, Behra P, Pontalier P-Y. Membrane filtration applied to the purification of sugarcane bagasse mild alkaline extracts. Clean Technol 2023;5:518–30. https://doi.org/10.3390/cleantechnol5020027.

[33] Doan NTT, Lai QD. Ultrafiltration for recovery of rice protein: fouling analysis and technical assessment. Innov Food Sci Emerg Technol 2021;70:102692. https://doi.org/10.1016/j.ifset.2021.102692.

[34] Wang Y, Tibbetts S, McGinn P. Microalgae as sources of high-quality protein for human food and protein supplements. Foods 2021;10:3002. https://doi.org/10.3390/foods10123002.

[35] Bradford MM. A rapid and sensitive method for the quantitation of microgram quantities of protein utilizing the principle of protein-dye binding. Anal Biochem 1976;72:248–54. https://doi.org/10.1016/0003-2697(76)90527-3.

[36] S. Van Wychen and L.M.L. Laurens, Determination of Total Carbohydrates in Algal Biomass, Laboratory Analytical Procedure (LAP), National Renewable Energy Laboratory (NREL), Golden, CO, USA, 2013. ⟨www.nrel.gov/publications⟩.

[37] Blumenkrantz N, Asboe-Hansen G. New method for quantitative determination of uronic acids. Anal Biochem 1973;54:484–9. https://doi.org/10.1016/0003-2697(73)90377-1.

[38] Delran P, Frances C, Guihéneuf F, Peydecastaing J, Pontalier P-Y, Barthe L. Tetraselmis suecica biofilm cell destruction by high-pressure homogenization for protein extraction. Bioresour Technol Rep 2023;21:101372. https://doi.org/10.1016/j.biteb.2023.101372.

[39] Pereira H, Silva J, Santos T, Gangadhar KN, Raposo A, Nunes C, Coimbra MA, Gouveia L, Barreira L, Varela J. Nutritional potential and toxicological evaluation of tetraselmis sp. CTP4 microalgal biomass produced in industrial photobioreactors. Molecules 2019;24:3192. https://doi.org/10.3390/molecules24173192.

[40] Delran P, Frances C, Peydecastaing J, Pontalier P-Y, Guihéneuf F, Barthe L. Cell destruction level and metabolites green-extraction of Tetraselmis suecica by low and intermediate frequency ultrasound. Ultrason Sonochem 2023;98:106492. https://doi.org/10.1016/j.ultsonch.2023.106492.

[41] Becker B, Melkonian M, Kamerling JP. The Cell Wall (theca) of Tetraselmis Striata (chlorophyta): macromolecular composition and structural elements of the complex polysaccharides. J Phycol 1998;34:779–87. https://doi.org/10.1046/j.1529-8817.1998.340779.x.

[42] Patel AK, Albarico FPJB, Perumal PK, Vadrale AP, Nian CT, Chau HTB, Anwar C, Wani HM ud din, Pal A, Saini H, Ha LH, Senthilkumar B, Tsang Y-S, Chen C-W, Dong C-D, Singhania RR. Algae as an emerging source of bioactive pigments. Bioresour Technol 2022;351:126910. https://doi.org/10.1016/j.biortech.2022.126910.

[43] Volkman JK, Jeffrey SW, Nichols PD, Rogers GI, Garland CD. Fatty acid and lipid composition of 10 species of microalgae used in mariculture. J Exp Mar Biol Ecol 1989;128:219–40. https://doi.org/10.1016/0022-0981(89)90029-4.

[44] Safi C, Cabas Rodriguez L, Mulder WJ, Engelen-Smit N, Spekking W, van den Broek LAM, Olivieri G, Sijtsma L. Energy consumption and water-soluble protein release by cell wall disruption of Nannochloropsis gaditana. Bioresour Technol 2017;239:204–10. https://doi.org/10.1016/j.biortech.2017.05.012.

[45] Xie Y, Ho S-H, Chen C-NN, Chen C-Y, Jing K, Ng I-S, Chen J, Chang J-S, Lu Y. Disruption of thermo-tolerant Desmodesmus sp. F51 in high pressure homogenization as a prelude to carotenoids extraction. Biochem Eng, J 2016;109:243–51. https://doi.org/10.1016/j.bej.2016.01.003.

[46] Fernández A, Riera FA. Membrane fractionation of a β-Lactoglobulin Tryptic Digest: effect of the hydrolysate concentration. Ind Eng Chem Res 2012;51:15738–44. https://doi.org/10.1021/ie302376g.

[47] S. Obeid, Ecodesign process for microalgae fractionation: use of supercritical CO2, membrane technology and low frequency ultrasounds, Doctoral dissertation, Institut National Polytechnique de Toulouse, 2018. ⟨https://oatao.univ-toulouse.fr/24643/⟩ (accessed November 27, 2022).

[48] Wan Osman WNA, Mat Nawi NI, Samsuri S, Bilad MR, Khan AL, Hunaepi H, Jaafar J, Lam MK. Ultra low-pressure filtration system for energy efficient microalgae filtration. Heliyon 2021;7:e07367. https://doi.org/10.1016/j.heliyon.2021.e07367.

[49] Liu S, Rouquié C, Frappart M, Szymczyk A, Rabiller-Baudry M, Couallier E. Separation of lipids and proteins from clarified microalgae lysate: the effect of lipid-protein interaction on the cross-flow and shear-enhanced microfiltration performances. Sep Purif Technol 2024;328:124985. https://doi.org/10.1016/j.seppur.2023.124985.

[50] Rossignol N, Vandanjon L, Jaouen P, Quéméneur F. Membrane technology for the continuous separation microalgae/culture medium: compared performances of cross-flow microfiltration and ultrafiltration. Aquac Eng 1999;20:191–208. https://doi.org/10.1016/S0144-8609(99)00018-7.

[51] Jönsson A-S. Influence of shear rate on the flux during ultrafiltration of colloidal substances. J Membr Sci 1993;79:93–9. https://doi.org/10.1016/0376-7388(93)85020-W.

[52] Soydemir G, Gurol MD, Hocaoğlu SM, Karagündüz A. Fouling mechanisms of membrane filtration of mixed microalgal biomass grown in wastewater. Water Sci Technol 2020;81:2127–39. https://doi.org/10.2166/wst.2020.268.

[53] Antón E, Álvarez JR, Palacio L, Prádanos P, Hernández A, Pihlajamäki A, Luque S. Ageing of polyethersulfone ultrafiltration membranes under long-term exposures to alkaline and acidic cleaning solutions. Chem Eng Sci 2015;134:178–95. https://doi.org/10.1016/j.ces.2015.04.023.

[54] Tsehaye MT, Velizarov S, Van Der Bruggen B. Stability of polyethersulfone membranes to oxidative agents: a review. Polym Degrad Stab 2018;157:15–33. https://doi.org/10.1016/j.polymdegradstab.2018.09.004.

[55] Shoshaa R, Ashfaq MY, Al-Ghouti MA. Recent developments in ultrafiltration membrane technology for the removal of potentially toxic elements, and enhanced antifouling performance: a review. Environ Technol Innov 2023;31:103162. https://doi.org/10.1016/j.eti.2023.103162.